

Beyond Diamond: Interpretable Machine Learning Discovery of Coherent Quantum Defect Hosts in Semiconductors

Mohammed Mahshook and Rudra Banerjee

Department of Physics and Nanotechnology, SRM Institute of Science and Technology, Kattankulathur, Tamil Nadu, 603203, India

(*rudrab@srmist.edu.in)

(Dated: June 5, 2025)

Quantum point defects in wide bandgap semiconductors—such as the nitrogen-vacancy (NV) center in diamond—are leading candidates for solid-state spin qubits due to their long coherence times and optically addressable spin states. Yet, identifying host materials capable of supporting such deep-level defects remains a significant challenge, owing to the complex interplay between chemical composition, crystal structure, and electronic environment. Here, we present a scalable, interpretable machine learning framework that combines density functional theory (DFT)-informed descriptors with a structure-agnostic ensemble model to predict quantum-compatible defect-host materials. Trained on a curated dataset from the Materials Project and ICSD, our model achieves a high Matthews correlation coefficient ($MCC > 0.95$) and assigns confidence scores to guide prioritization of candidates. First-principles calculations of coherence-relevant properties, including static dielectric constants and defect formation energetics, validate key predictions. While high dielectric response is a necessary but not sufficient condition for spin coherence, our model successfully recovers known hosts such as diamond and SiC, and reveals previously overlooked candidates such as WS_2 , MgO, CaS and TiO_2 . This approach establishes a robust path for discovering next-generation quantum materials, bridging data-driven screening with physically interpretable design principles.

I. INTRODUCTION

The field of quantum information science (QIS) has witnessed remarkable progress over the past decade, catalyzing transformative developments across quantum computing, communication, and sensing[1–4]. Central to the realization of scalable quantum technologies is the identification of robust qubit platforms[5]. While architectures based on ultracold atoms[6–8], superconducting circuits[9–11], and photonic systems[12, 13] have demonstrated significant promise, they often face challenges in achieving the stringent requirements of practical deployment. These requirements include ultra-long spin coherence times[14], high-fidelity state control and readout[15–17], and seamless integration with fault-tolerant architectures[18–21].

Solid-state spin defects in wide bandgap semiconductors have emerged as compelling candidates for quantum technologies. Among them, the negatively charged nitrogen-vacancy (NV^-) centre in diamond stands out, offering optically addressable spin states with exceptional coherence times at room temperature[22, 23]. The success of NV centres has spurred efforts to engineer analogous quantum defects in alternative host materials such as silicon carbide (SiC)[24], hexagonal boron nitride (hBN)[25], and certain transition metal dichalcogenides (TMDs)[26, 27]. However, designing suitable host-defect systems remains inherently complex: ideal defects must exhibit well-isolated mid-gap levels, structural and electronic stability, long spin coherence, optical addressability, and thermodynamic favorability under realistic growth conditions[28–30].

The search for new quantum defect hosts is further complicated by the immense size of the chemical composition space. Even under basic constraints such as charge neutrality and electronegativity balance, the number of stoichiometrically valid binary compounds exceeds three million[31]. Beyond composition, multiple crystal structures per composition and the strong structure-dependence of key properties, such as spin-orbit coupling and band gap, pose additional challenges[29, 31]. Conventional high-throughput screening[32, 33] and experimental approaches[34] are computationally expensive and largely limited to experimentally reported structures, leaving vast regions of the chemical landscape unexplored.

Machine learning (ML) offers a scalable and efficient alternative, often accelerating discovery by orders of magnitude relative to traditional workflows[35]. However, two major hurdles limit its application to quantum defect discovery: the scarcity of well-characterized training data and the difficulty of crafting physically meaningful descriptors[36]. Because the physics of defect formation and spin coherence is still emerging, representing materials in a way that

captures quantum defect compatibility remains a formidable challenge[30, 37].

In this work, we address these limitations by developing a structure-agnostic, interpretable machine learning framework to efficiently discover quantum-compatible deep centres across broad chemical spaces. By integrating density functional theory (DFT)-informed descriptors with a heterogeneous ensemble of machine learning models, we offer a scalable strategy to accelerate the discovery of quantum materials beyond traditional heuristics.

II. METHODS

The desired properties that NV-centre-like defects in semiconductors exhibit often arise from the defect acting as a deep-level centre. Quantum information encoded in the electronic spin states of such defects experiences minimal environmental perturbations if the host satisfies certain conditions, leading to long spin coherence times. The spin-lattice relaxation time (T_1) and the spin-spin relaxation time (T_2) collectively quantify these properties: T_1 measures the timescale for spin relaxation via phonon-mediated processes, whereas T_2 characterizes decoherence due to environmental interactions. Since $T_2 < 0.5T_1$ in practice [38], maximizing T_2 is crucial for quantum applications. Higher T_2 times are required for efficient qubit initialization, manipulation, and readout. While T_1 is strongly influenced by defect energy levels [39], T_2 can be effectively engineered via host material properties [28].

A. Database Creation

We constructed a labeled dataset by intersecting the Materials Project [40] and ICSD [41] databases. To ensure thermodynamical stability, only phases with Energy above the convex hull (E_{Hull}) less than 0.2 eV were considered. Positive class candidates were screened by applying the following coherence-relevant filters: (a) Bandgap $\Delta E_g > 0.5$ eV to ensure optical transitions and account for PBE underestimation; (b) only elements with stable nuclear spin-zero isotopes; (c) exclusion of magnetic materials; and (d) exclusion of polar space groups to suppress inhomogeneous electric field noise[28–30].

Negative classes are defined by contrasting conditions, materials that are simultaneously metallic, magnetic, and polar, and contains at least one element with non-zero nuclear spin in the composition. Polymorphs were consolidated into a single entry to avoid duplicated instances. We note that despite the labelling criteria being structure dependent, there were no overlapping entries between classes.

B. Feature Engineering

Each material composition was represented using descriptors inspired by Meredig *et al.*[42] and Ward *et al.* [43], augmented with features relevant to defect physics. Feature categories included: (a) elemental fraction vectors; (b) valence electron counts; (c) stoichiometric norms (I_n norms); and (d) atomic orbital-derived HOMO, LUMO, and band centre estimates. Although stoichiometric features exhibited high inter-correlation, they were retained due to their positive contribution to model’s predictive power. Feature relevance was validated using permutation importance and accumulated local effects (ALE) analysis [44].

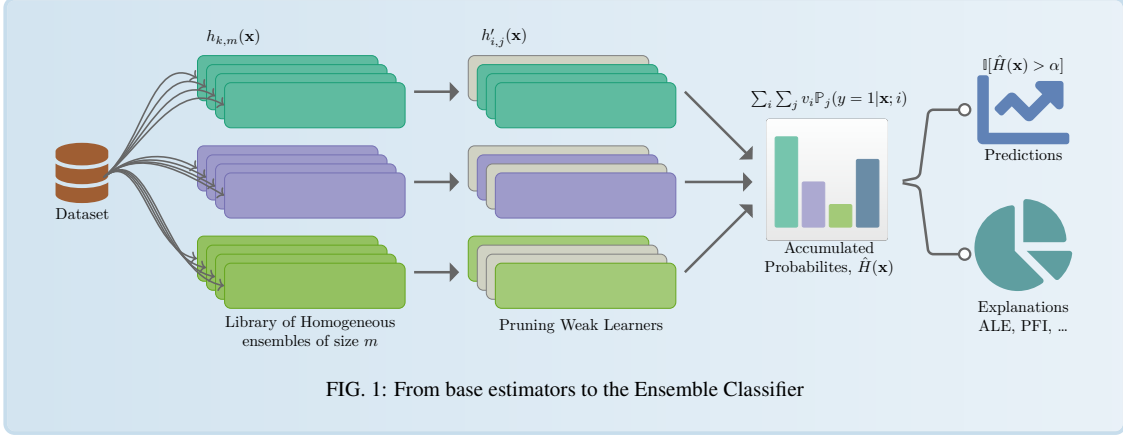
C. Model Building

To enable robust predictions for quantum-compatible host materials, we developed a heterogeneous ensemble model from homogeneous ensembles of base models[45] Logistic Regression (LR), Stochastic Gradient Descent Classifier (SGC), Support Vector Classifier (SVC), Random Forests Classifier (RFC), Gradient Boosting (GB), k -nearest neighbours (KNN), and Bernoulli Naive Bayes Classifier (NBC). While these models achieved similar performance on the test set (TABLE (I)), they learned distinct decision boundaries, often relying on different-sometimes spurious feature relationships.

We formalized this phenomenon using the *Rashomon set* framework[46], which defines the family of near-optimal models:

$$\mathcal{R}(\epsilon, f^*, \mathcal{F}) = \{f \in \mathcal{F} \mid L(f) \leq (1 + \epsilon)L(f^*)\}, \quad (1)$$

where f^* is the best-performing model in hypothesis space \mathcal{F} , and L is the loss function. To account for data



imbalance, we define the Rashomon set using the *Matthews Correlation Coefficient (MCC)*:

$$\mathcal{R}(\epsilon, f^*, \mathcal{F}) = \{f \in \mathcal{F} \mid \text{MCC}(f) \geq \text{MCC}(f^*) - \epsilon\}. \quad (2)$$

We identified two such sets: \mathcal{F}_1 , anchored by SVC and containing RFC, GB, and NBC; and \mathcal{F}_2 , centred on SGC and LR. Despite similar MCC scores, these sets learned conflicting feature dependencies. Thus, relying on the predictions of an individual model on unseen data could lead to errors.

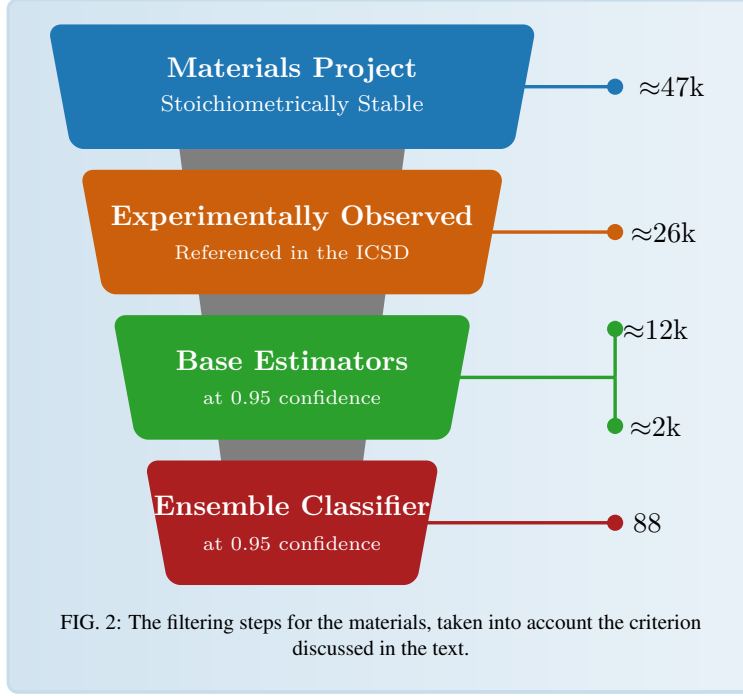
To resolve this, we introduce a novel, interpretability-driven ensemble construction strategy. By combining Rashomon analysis with explainable AI methods-permutation feature importance (PFI), partial dependence, and accumulated local effects (ALE)-we identify robust, generalizable patterns while suppressing model-specific artefacts. A schematic of the process is shown in FIG. (1).

The dataset was split into train, test and validation sets in the ratio 7:2:1. Each homogeneous ensemble comprises n models trained with the same sampling strategy, by under-sampling the positive class to balance the training data. The ensemble constituents were then pruned dynamically by evaluating the performance of the base estimators on the validation set. Two ensemble aggregation strategies were implemented:

- (a) **Mean Voting:** Final predictions were determined by averaging the predicted probabilities across base learners.
- (b) **Constrained Voting:** A material was classified as positive only if *every* base homogeneous ensemble assigned a mean probability greater than 0.5. This approach promoted diversity and robustness, while ensemble interpretability was retained using via XAI methods, ALE, PDP, and PFI. Hyperparameter optimization was conducted via grid search, using the Matthews correlation coefficient (MCC)[47] as the primary evaluation metric, with five-fold stratified cross-validation using the formula:

$$\frac{TP \cdot TN - FP \cdot FN}{\sqrt{(TP + FP)(TP + FN)(TN + FP)(TN + FN)}} \quad (3)$$

where TP , FP , TN and FN stands for true positive, false positive, true negative and false negative prediction. FIG. (2) shows the combined database creation and model building. Our final ensemble selectively aggregates models with consistent physical reasoning, identifying complimentary trends from the base learners, improving both generalization and trustworthiness.



Details on model variance, learning curves, pruning strategies, and full feature evaluation are provided in the Supplementary Information.

D. First-Principles Calculations

To support machine learning predictions, density functional theory (DFT) calculations were performed using the Vienna Ab-initio Simulation Package (VASP) [48, 49], employing the projector augmented wave (PAW) method [50] and the PBE generalized gradient approximation functional [51]. Plane-wave kinetic energy cutoffs of 520 eV were employed, and structures were relaxed until forces were below 0.01 eV/Å. Monkhorst-Pack k -point grids with at least $5 \times 5 \times 5$ meshes were used for primitive cells.

Defect formation energies $E_f[D^q]$ were computed in $2 \times 2 \times 2$ supercells using the Freysoldt–Neugebauer–Van de Walle (FNV) correction scheme [52] to mitigate finite-size effects in charged systems as [53, 54]:

$$E_f[D^q] = E_{\text{tot}}[D^q] - E_{\text{tot}}[\text{bulk}] - \sum_i n_i \mu_i + q(E_F + \epsilon_v) + E_{\text{corr}}, \quad (4)$$

where $E_{\text{tot}}[D^q]$ and $E_{\text{tot}}[\text{bulk}]$ are the total energies of the defective and pristine supercells, n_i and μ_i denote the number and chemical potential of species i , E_F is the Fermi level referenced to the valence band maximum ϵ_v , and E_{corr} accounts for image charge corrections.

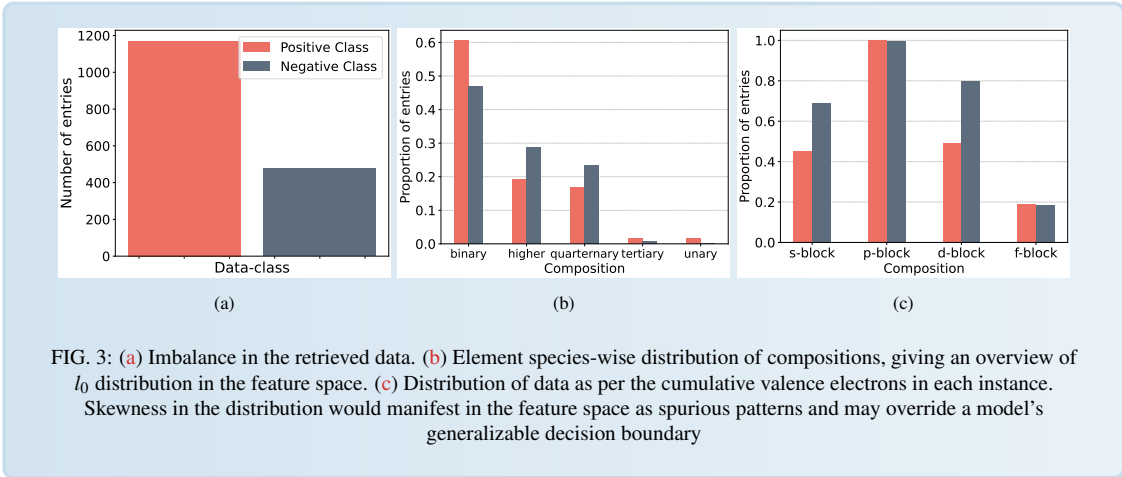
Static dielectric tensors were calculated using density functional perturbation theory (DFPT) [55, 56], separating the electronic (ϵ_∞) and ionic (ϵ_{ion}) contributions. Higher total dielectric constants, particularly those dominated by ionic contributions, are correlated with improved spin coherence times [28]. The mid-level defect site is computed as implemented in pymatgen[40].

Metrics	SGC	SVC	RFC	KNN	LR	NBC	GBC	EC*
Train Precision	0.960	1.000	1.000	1.000	0.937	0.993	0.998	1.000
Test Precision	0.941	0.992	0.984	0.850	0.937	0.992	0.976	0.992
Train Recall	1.000	1.000	1.000	1.000	0.981	0.992	1.000	1.000
Test Recall	0.996	0.992	1.000	0.934	0.984	0.984	1.000	1.000
Train F1 Score	0.979	1.000	1.000	1.000	0.959	0.992	0.998	1.000
Test F1 Score	0.968	0.992	0.992	0.890	0.960	0.988	0.988	0.996
Train MCC	0.925	1.000	1.000	1.000	0.850	0.973	0.995	1.000
Test MCC	0.882	0.971	0.971	0.566	0.851	0.956	0.956	0.985

TABLE I: Performance of individual base models and the ensemble classifier (EC*) on training and test datasets.

III. RESULTS

The dataset, curated from the Materials Project, was inherently skewed toward the positive class due to constraints such as nuclear spin-zero elements. To avoid sampling bias and ensure robust model generalization, we analyzed feature space distributions (FIG. (3)). Despite compositional restrictions in the positive class, element-wise and va-



lence electron distributions remained balanced across classes. Redundant entries and duplicates were removed, and compositions were featurized into 232-dimensional vectors using Matminer tools to represent electronic and chemical environments.

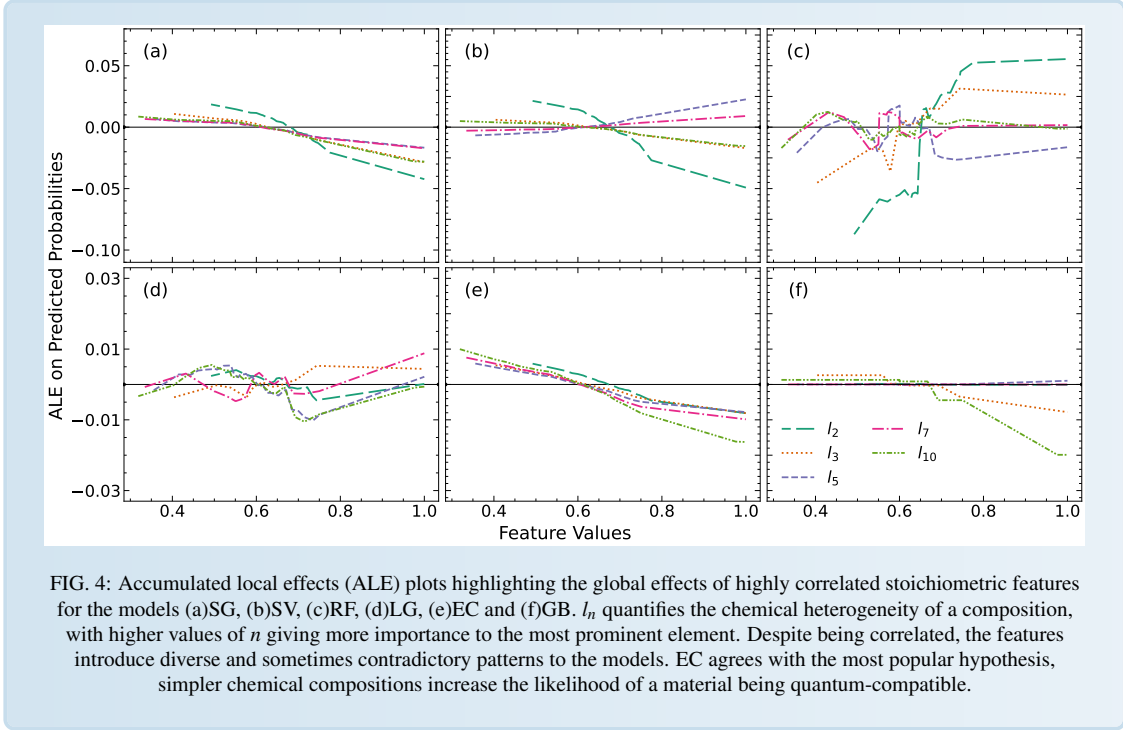
A. Model Validation and Learning Behavior

The ensemble model demonstrated robust classification performance, achieving a Matthews correlation coefficient (MCC) of ≈ 0.99 , with almost perfect precision, recall and f1 score on the held-out test set TABLE (I). The Ensemble Classifier (EC) consistently outperformed any individual base learner, underscoring the effectiveness of the heterogeneous ensemble strategy.

B. Feature Interpretation and Decision Boundaries

While individual models struggled to identify a uniform decision boundary, and often learned spurious patterns from the data, (FIG. (4)), EC identified trends that are more precise and uniform across data distributions. Subsets of the feature space where the individual models contradicted, EC's learning patterns were more robust and aligned with well-established patterns characterising quantum compatibility. The accumulated local effects (ALE) plots indicated that increasing bandgap and reducing elemental complexity improved the probability of positive classification (FIG.

(4)). These trends align with physical expectations: wide bandgaps suppress mid-gap phonon modes, and chemical homogeneity reduces decoherence from nuclear spins. In addition to these, EC favours completely filled s orbitals in the valence shells for positive classification. Partially filled d and f orbitals in the composition had a detrimental effect.



C. Screening of Unexplored Materials

We applied the ensemble model to a filtered subset of the Materials Project database, consisting of approximately 45,000 compounds previously uncharacterized for quantum applications. Predictions were made using the constrained voting strategy described in Methods. At a confidence threshold of 0.95, the model identified 88 candidate materials, predominantly oxides, sulfides, and carbides (FIG. (5)). Among the high-confidence candidates were known quantum defect hosts such as diamond (C), silicon carbide (SiC), Zinc Oxide (ZnO), Zinc Sulfide (ZnS) and Tungsten Disulfide (WS₂), validating model fidelity. More significantly, the model uncovered previously overlooked families such as transition metal dichalcogenides (e.g., PtS₂, HfS₂) layered sulfides (e.g., SnS₂, TiS₂) and oxides (TiO₂, PbWO₄) etc, suggesting broader chemical platforms for solid-state spin qubits. Further, materials like MgO, CaO, WO₃, SiO₂, CaS and S, that were theoretically shown to have promising host attributes[57, 58] were also identified at the same confidence level indicating the model's versatility in identifying promising candidates from diverse chemical landscapes.

D. First-Principles Validation of Predictions

To validate the physical plausibility of the predicted candidates, we computed static dielectric tensors (ϵ_{total}) using density functional perturbation theory (DFPT). Materials with high dielectric constants are expected to exhibit longer T_2 coherence times due to suppression of electric field noise[28].

FIG. (6) shows a positive correlation between dielectric constant and experimentally measured T_2 times for benchmark hosts. Newly identified candidates such as PbWO₄, HfS₂, and TiO₂ exhibit ϵ_{total} values comparable to or exceeding those of SiC and WS₂, suggesting strong potential for quantum defect applications.

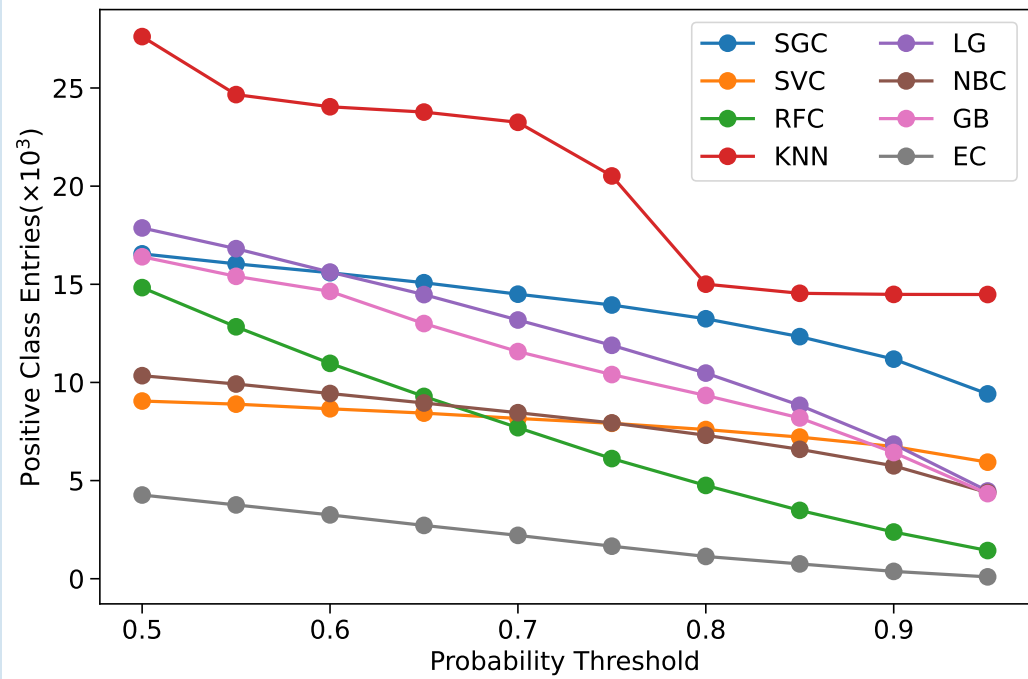


FIG. 5: Number of predicted positive entries from the Materials Project database as a function of confidence thresholds for each of the models considered.

Furthermore, analysis of the ionic and electronic components of the dielectric response indicated that materials with dominant ionic contributions favored longer T_2 times, consistent with prior theoretical predictions [30].

For example, the calculated defect spectrum of oxygen vacancies in TiO_2 features deep, well-isolated states between 2.40 and 2.65 eV above the valence band maximum, with minimal hybridization near the band edges. Such deep and energetically isolated levels, combined with moderate DOS (1-4 states/eV), with $\epsilon_0 \approx 59$ in-plane and ≈ 26 out-of-plane are known to suppress charge and phonon noise—key sources of spin decoherence [29]. The absence of band-tail states and narrow energy spread further minimize spectral diffusion, making oxygen-deficient TiO_2 a promising platform for coherent spin qubits.

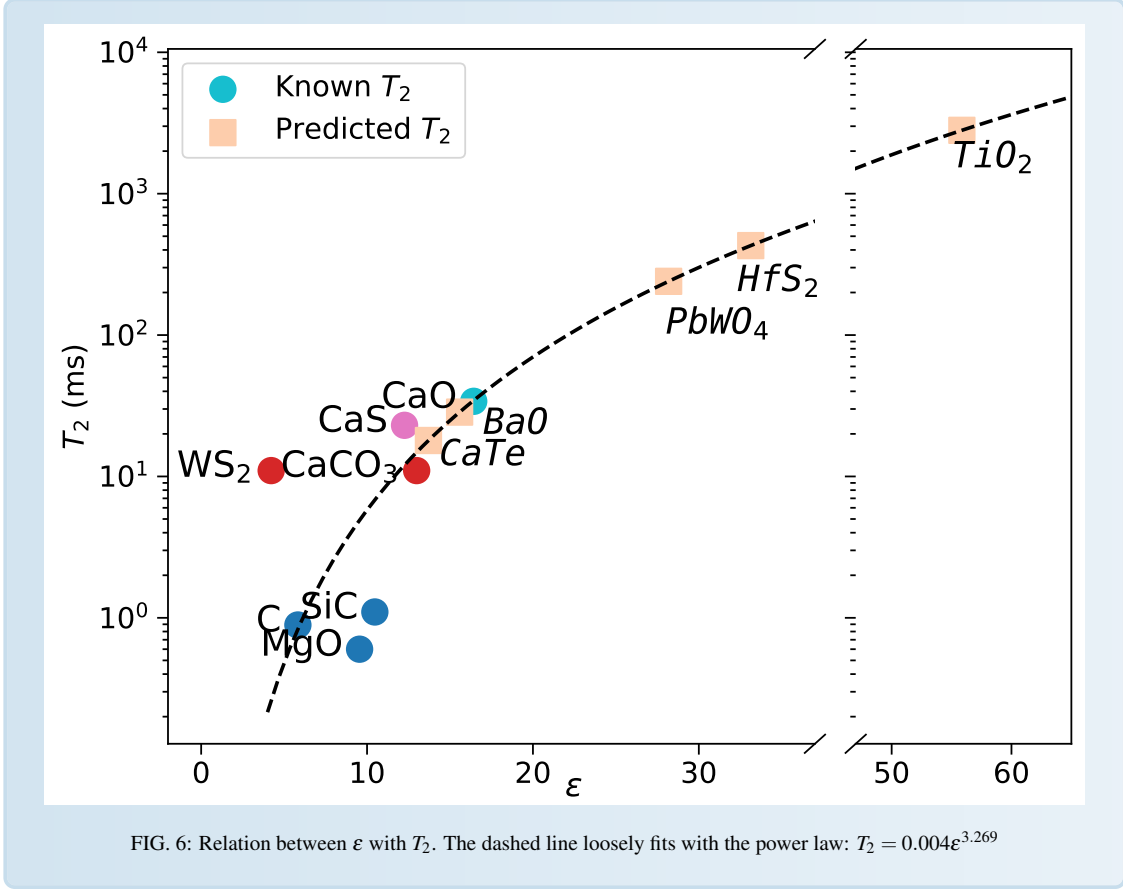
E. Emerging Trends and Implications

The ensemble learning framework not only recovered known quantum hosts but also predicted chemically diverse families, including layered sulfides and oxides with high dielectric screening and nonpolar structures. This highlights the advantage of a structure-agnostic approach capable of extrapolating beyond conventional heuristics.

Overall, these results demonstrate that machine learning, when informed by quantum coherence-relevant descriptors and first-principles validation, offers a scalable strategy for discovering next-generation quantum materials.

DISCUSSION

Our integrated machine learning and first-principles framework presents a scalable and interpretable strategy for identifying coherent quantum defect hosts across the vast chemical space of inorganic semiconductors. In contrast to prior heuristic or structure-constrained approaches, our structure-agnostic ensemble model achieves high predictive



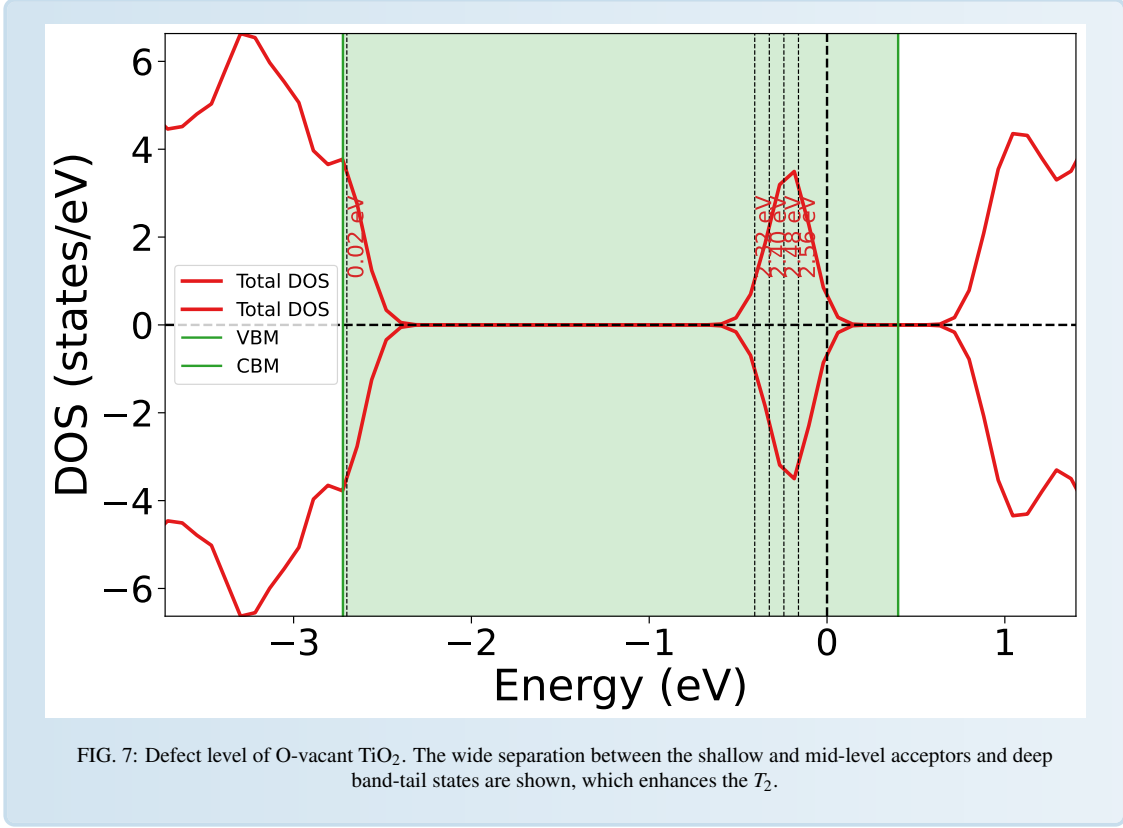
performance (MCC > 0.95), while maintaining transparency through feature relevance and accumulated local effects. Here, we would like to stress that the DFT calculations performed here does not confirm that the systems will be a good qubit material. We need to incorporate SOC calculations and phonon calculation for confirmations. High ϵ is a necessary condition for materials to show good qubit properties and our DFT calculation merely confirms that our machine learning models picks up materials that is in confirmation with that.

Beyond reproducing known hosts like diamond and SiC, the model successfully identifies chemically diverse candidates such as WS_2 , PbWO_4 , HfS_2 , and TiO_2 , which exhibit favorable physical attributes—wide bandgaps, non-polarity, and high dielectric constants—validated via first-principles calculations. The observed correlation between dielectric screening and T_2 coherence times further supports the physical fidelity of the predictions.

The model also uncovers broader coherence-preserving design principles, such as the role of ionic character, elemental simplicity, and reduced spin noise, underscoring the capacity of data-driven methods to capture complex quantum-defect compatibility without explicit defect-level enumeration.

Compared to prior high-throughput or descriptor-based screenings [59–61], our approach offers three key advantages: (i) generalizability across chemistries beyond fixed structural families, (ii) integration of coherence-relevant descriptors beyond conventional bandgap filtering, and (iii) enhanced interpretability through transparent feature attribution. This positions our model as a robust and scalable alternative for defect discovery across previously inaccessible chemical spaces.

Future directions include incorporating synthesis feasibility, defect-specific optical and spin properties, and extending the framework to targeted color centres or tunable 2D materials. Altogether, this work bridges machine learning and quantum materials theory to accelerate the discovery of next-generation quantum platforms beyond traditional design boundaries.



DATA AVAILABILITY

All data used in the work is available in supplementary section and github.

CODE AVAILABILITY

Except VASP, all other codes are open source software, available in the website. The codes developed by us are available in github.

AUTHOR CONTRIBUTIONS

MM: Conceptualization, Data Curation, Formal Analysis, Software, Visualization, Writing – Original Draft Preparation.

RB: Conceptualization, Methodology, Resources, Supervision, Validation, Writing – Review & Editing

-
- [1] Abhishek Purohit, Maninder Kaur, Zeki Can Seskir, Matthew T Posner, and Araceli Venegas-Gomez. Building a quantum-ready ecosystem. *IET Quantum Communication*, 5(1):1–18, 2024.
 - [2] David Barral, F Javier Cardama, Guillermo Díaz-Camacho, Daniel Faílde, Iago F Llovo, Mariamo Mussa-Juane, Jorge

- Vázquez-Pérez, Juan Villasuso, César Piñeiro, Natalia Costas, et al. Review of distributed quantum computing: from single qpu to high performance quantum computing. *Computer Science Review*, 57:100747, 2025.
- [3] Pharnam Bakhshinezhad, Mohammad Mehboudi, Carles Roch I Carceller, and Armin Tavakoli. Scalable entanglement certification via quantum communication. *PRX Quantum*, 5(2):020319, 2024.
 - [4] David DeMille, Nicholas R Hutzler, Ana Maria Rey, and Tanya Zelevinsky. Quantum sensing and metrology for fundamental physics with molecules. *Nature Physics*, 20(5):741–749, 2024.
 - [5] Eunmi Chae, Joonhee Choi, and Junki Kim. An elementary review on basic principles and developments of qubits for quantum computing. *Nano Convergence*, 11(1):11, 2024.
 - [6] Hartmut Häffner, Christian F Roos, and Rainer Blatt. Quantum computing with trapped ions. *Physics reports*, 469(4):155–203, 2008.
 - [7] MA Weber, MF Gely, RK Hanley, TP Harty, AD Leu, CM Löschnauer, DP Nadlinger, and DM Lucas. Robust and fast microwave-driven quantum logic for trapped-ion qubits. *Physical Review A*, 110(1):L010601, 2024.
 - [8] Jad C Halimeh, Monika Aidelsburger, Fabian Grusdt, Philipp Hauke, and Bing Yang. Cold-atom quantum simulators of gauge theories. *Nature Physics*, pages 1–12, 2025.
 - [9] John Clarke and Frank K Wilhelm. Superconducting quantum bits. *Nature*, 453(7198):1031–1042, 2008.
 - [10] Anasua Chatterjee, Paul Stevenson, Silvano De Franceschi, Andrea Morello, Nathalie P de Leon, and Ferdinand Kuemmeth. Semiconductor qubits in practice. *Nature Reviews Physics*, 3(3):157–177, 2021.
 - [11] Haining Pan, Sankar Das Sarma, and Chun-Xiao Liu. Rabi and ramsey oscillations of a majorana qubit in a quantum dot-superconductor array. *Physical Review B*, 111(7):075416, 2025.
 - [12] Srujan Meesala, David Lake, Steven Wood, Piero Chiappina, Changchun Zhong, Andrew D Beyer, Matthew D Shaw, Liang Jiang, and Oskar Painter. Quantum entanglement between optical and microwave photonic qubits. *Physical Review X*, 14(3):031055, 2024.
 - [13] Yu-Ping Liu, Zhong-Wen Ou, Tian-Xiang Zhu, Ming-Xu Su, Chao Liu, Yong-Jian Han, Zong-Quan Zhou, Chuan-Feng Li, and Guang-Can Guo. A millisecond integrated quantum memory for photonic qubits. *Science Advances*, 11(13):eadu5264, 2025.
 - [14] John Preskill. Quantum computing in the nisq era and beyond. *Quantum*, 2:79, 2018.
 - [15] Yutaro Akahoshi, Kazunori Maruyama, Hirotaka Oshima, Shintaro Sato, and Keisuke Fujii. Partially fault-tolerant quantum computing architecture with error-corrected clifford gates and space-time efficient analog rotations. *PRX quantum*, 5(1):010337, 2024.
 - [16] CM Löschnauer, J Mosca Toba, AC Hughes, SA King, MA Weber, R Srinivas, R Matt, R Nourshargh, DTC Allcock, CJ Ballance, et al. Scalable, high-fidelity all-electronic control of trapped-ion qubits. *arXiv preprint arXiv:2407.07694*, 2024.
 - [17] P-Y Song, J-F Wei, Peng Xu, L-L Yan, M Feng, Shi-Lei Su, and Gang Chen. Fast realization of high-fidelity nonadiabatic holonomic quantum gates with a time-optimal-control technique in rydberg atoms. *Physical Review A*, 109(2):022613, 2024.
 - [18] Earl T Campbell, Barbara M Terhal, and Christophe Vuillot. Roads towards fault-tolerant universal quantum computation. *Nature*, 549(7671):172–179, 2017.
 - [19] Benedikt Fauseweh. Quantum many-body simulations on digital quantum computers: State-of-the-art and future challenges. *Nature Communications*, 15(1):2123, 2024.
 - [20] Nathalie P De Leon, Kohei M Itoh, Dohun Kim, Karan K Mehta, Tracy E Northup, Hanhee Paik, BS Palmer, Nitin Samarth, Sorawis Sangtawesin, and David W Steuerman. Materials challenges and opportunities for quantum computing hardware. *Science*, 372(6539):eabb2823, 2021.
 - [21] Diana Franklin and Frederic T Chong. Challenges in reliable quantum computing. *Nano, quantum and molecular computing: implications to high level design and validation*, pages 247–266, 2004.
 - [22] NB Manson, JP Harrison, and MJ Sellars. Nitrogen-vacancy center in diamond: Model of the electronic structure and associated dynamics. *Physical Review B—Condensed Matter and Materials Physics*, 74(10):104303, 2006.
 - [23] Laura Orphal-Kobin, Cem Güney Torun, Julian M Bopp, Gregor Pieplow, and Tim Schröder. Coherent microwave, optical, and mechanical quantum control of spin qubits in diamond. *Advanced Quantum Technologies*, 8(2):2300432, 2025.
 - [24] Stephanie Simmons. Scalable fault-tolerant quantum technologies with silicon color centers. *PRX quantum*, 5(1):010102, 2024.
 - [25] Marina Radulaski, Matthias Widmann, Matthias Niethammer, Jingyuan Linda Zhang, Sang-Yun Lee, Torsten Rendler, Konstantinos G Lagoudakis, Nguyen Tien Son, Erik Janzen, and Takeshi Ohshima. Scalable quantum photonics with single color centers in silicon carbide. *Nano letters*, 17(3):1782–1786, 2017.
 - [26] Song Li, Gergő Thiering, Péter Udvarhelyi, Viktor Ivády, and Adam Gali. Carbon defect qubit in two-dimensional ws2. *Nature communications*, 13(1):1210, 2022.
 - [27] Yeonghun Lee, Yaoqiao Hu, Xiuyao Lang, Dongwook Kim, Kejun Li, Yuan Ping, Kai-Mei C Fu, and Kyeongjae Cho. Spin-defect qubits in two-dimensional transition metal dichalcogenides operating at telecom wavelengths. *Nature Communications*, 13(1):7501, 2022.
 - [28] Gary Wolfowicz, F Joseph Heremans, Christopher P Anderson, Shun Kanai, Hosung Seo, Adam Gali, Giulia Galli, and David D Awschalom. Quantum guidelines for solid-state spin defects. *Nature Reviews Materials*, 6(10):906–925, 2021.
 - [29] JR Weber, WF Koehl, JB Varley, Anderson Janotti, BB Buckley, CG Van de Walle, and David D Awschalom. Quantum

- computing with defects. *Proceedings of the National Academy of Sciences*, 107(19):8513–8518, 2010.
- [30] Austin M Ferrenti, Nathalie P de Leon, Jeff D Thompson, and Robert J Cava. Identifying candidate hosts for quantum defects via data mining. *npj Computational Materials*, 6(1):126, 2020.
 - [31] DW Davies, KT Butler, AJ Jackson, A Morris, JM Frost, JM Skelton, and A Walsh. Computational screening of all stoichiometric inorganic materials. *chem* 2016, 1 (4), 617–627.
 - [32] Rodrick Kuate Defo, Haimi Nguyen, Mark JH Ku, and Trevor David Rhone. Methods to accelerate high-throughput screening of atomic qubit candidates in van der waals materials. *Journal of Applied Physics*, 129(22), 2021.
 - [33] Yihuang Xiong, Céline Bourgois, Natalya Sheremetyeva, Wei Chen, Diana Dahliah, Hanbin Song, Jiongzi Zheng, Sinéad M Griffin, Alp Sipahigil, and Geoffroy Hautier. High-throughput identification of spin-photon interfaces in silicon. *Science Advances*, 9(40):eadh8617, 2023.
 - [34] Joel Davidsson, Mykyta Onizhuk, Christian Vorwerk, and Giulia Galli. Discovery of atomic clock-like spin defects in simple oxides from first principles. *Nature Communications*, 15(1):4812, 2024.
 - [35] Yongfei Juan, Yongbing Dai, Yang Yang, and Jiao Zhang. Accelerating materials discovery using machine learning. *Journal of Materials Science & Technology*, 79:178–190, 2021.
 - [36] Chen Li and Kun Zheng. Methods, progresses, and opportunities of materials informatics. *InfoMat*, 5(8):e12425, 2023.
 - [37] Oliver Lerstøl Hebnes, Marianne Etzelmüller Bathen, Øyvind Sigmundson Schøyen, Sebastian G Winther-Larsen, Lasse Vines, and Morten Hjorth-Jensen. Predicting solid state material platforms for quantum technologies. *npj Computational Materials*, 8(1):207, 2022.
 - [38] Nir Bar-Gill, Linh M Pham, Andrejs Jarmola, Dmitry Budker, and Ronald L Walsworth. Solid-state electronic spin coherence time approaching one second. *Nature communications*, 4(1):1743, 2013.
 - [39] A Jarmola, VM Acosta, K Jensen, S Chemerisov, and D Budker. Temperature-and magnetic-field-dependent longitudinal spin relaxation in nitrogen-vacancy ensembles in diamond. *Physical review letters*, 108(19):197601, 2012.
 - [40] Anubhav Jain, Shyue Ping Ong, Geoffroy Hautier, Wei Chen, William Davidson Richards, Stephen Dacek, Shreyas Cholia, Dan Gunter, David Skinner, Gerbrand Ceder, et al. Commentary: The materials project: A materials genome approach to accelerating materials innovation. *APL materials*, 1(1), 2013.
 - [41] Dejan Zagorac, H Müller, S Ruehl, J Zagorac, and Silke Rehme. Recent developments in the inorganic crystal structure database: theoretical crystal structure data and related features. *Journal of applied crystallography*, 52(5):918–925, 2019.
 - [42] Bryce Meredig, Ankit Agrawal, Scott Kirklin, James E Saal, Jeff W Doak, Alan Thompson, Kunpeng Zhang, Alok Choudhary, and Christopher Wolverton. Combinatorial screening for new materials in unconstrained composition space with machine learning. *Physical Review B*, 89(9):094104, 2014.
 - [43] Logan Ward, Ankit Agrawal, Alok Choudhary, and Christopher Wolverton. A general-purpose machine learning framework for predicting properties of inorganic materials. *npj Computational Materials*, 2(1):1–7, 2016.
 - [44] Daniel W. Apley and Jingyu Zhu. Visualizing the effects of predictor variables in black box supervised learning models. *Journal of the Royal Statistical Society Series B: Statistical Methodology*, 82(4):1059–1086, 06 2020.
 - [45] Maryam Sabzevari, Gonzalo Martínez-Muñoz, and Alberto Suárez. Building heterogeneous ensembles by pooling homogeneous ensembles. *International Journal of Machine Learning and Cybernetics*, pages 1–8, 2022.
 - [46] Leo Breiman. Statistical modeling: The two cultures. *Quality control and applied statistics*, 48(1):81–82, 2003.
 - [47] Davide Chicco and Giuseppe Jurman. The Matthews correlation coefficient (mcc) should replace the roc auc as the standard metric for assessing binary classification. *BioData Mining*, 16(1):4, 2023.
 - [48] G. Kresse and J. Furthmüller. Efficient iterative schemes for ab initio total-energy calculations using a plane-wave basis set. *Phys. Rev. B*, 54(16):11169–11186, 1996.
 - [49] G. Kresse and D. Joubert. From ultrasoft pseudopotentials to the projector augmented-wave method. *Phys. Rev. B*, 59(3):1758–1775, 1999.
 - [50] P. E. Blöchl. Projector augmented-wave method. *Phys. Rev. B*, 50(24):17953–17979, 1994.
 - [51] J. P. Perdew, K. Burke, and M. Ernzerhof. Generalized gradient approximation made simple. *Phys. Rev. Lett.*, 77(18):3865–3868, 1996.
 - [52] C. Freysoldt, J. Neugebauer, and C. G. Van de Walle. Fully ab initio finite-size corrections for charged-defect supercell calculations. *Phys. Rev. Lett.*, 102(1):016402, 2009.
 - [53] S. B. Zhang and J. E. Northrup. Chemical potential dependence of defect formation energies in gaas: Application to ga self-diffusion. *Phys. Rev. Lett.*, 67(17):2339–2342, 1991.
 - [54] S. Lany and A. Zunger. Assessment of correction methods for the band-gap problem and for finite-size effects in supercell defect calculations: Case studies for zno and gaas. *Phys. Rev. B*, 78(23):235104, 2008.
 - [55] Stefano Baroni and Raffaele Resta. Ab initio calculation of the macroscopic dielectric constant in silicon. *Phys. Rev. B*, 33:7017–7021, 05 1986.
 - [56] M. Gajdoš, K. Hummer, G. Kresse, J. Furthmüller, and F. Bechstedt. Linear optical properties in the projector-augmented wave methodology. *Phys. Rev. B*, 73:045112, 01 2006.
 - [57] Shun Kanai, F Joseph Heremans, Hosung Seo, Gary Wolfowicz, Christopher P Anderson, Sean E Sullivan, Mykyta Onizhuk, Giulia Galli, David D Awschalom, and Hideo Ohno. Generalized scaling of spin qubit coherence in over 12,000 host materials. *Proceedings of the National Academy of Sciences*, 119(15):e2121808119, 2022.

- [58] Vrindaa Somjit, Joel Davidsson, Yu Jin, and Giulia Galli. An nv- center in magnesium oxide as a spin qubit for hybrid quantum technologies. *npj Computational Materials*, 11(1):74, 2025.
- [59] Viet-Anh Ha and Feliciano Giustino. High-throughput screening of 2d materials identifies p-type monolayer ws₂ as potential ultra-high mobility semiconductor. *npj Computational Materials*, 10(1), sep 2024.
- [60] Wu Liu, Ning Meng, Xiaomin Huo, Yao Lu, Yu Zhang, Xiaofeng Huang, Zhenqun Liang, Suling Zhao, Bo Qiao, Zhiqin Liang, Zheng Xu, and Dandan Song. Machine learning enables intelligent screening of interface materials towards minimizing voltage losses for p-i-n type perovskite solar cells. *Journal of Energy Chemistry*, 83:128–137, aug 2023.
- [61] Samad Razzaq and Kai S. Exner. Materials screening by the descriptor $g_{\max}(\eta)$: The free-energy span model in electrocatalysis. *ACS Catalysis*, 13(3):1740–1758, jan 2023.